COMPDYN 2025
10th ECCOMAS Thematic Conference on
Computational Methods in Structural Dynamics and Earthquake Engineering
M. Papadrakakis, M. Fragiadakis (eds.)
Rhodes Island, Greece, 15-18 June 2025

FIRST RESULTS OF THE APPLICATION OF A VISION-BASED METHODOLOGY FOR MONITORING DISPLACEMENTS DURING FULL-SCALE BUILDING SHAKE-TABLE TESTING

Laura Gioiella[1], Fabio Micozzi[1], Morgan McBain[2], Michele Morici[1], Alessandro Zona[1], Andrea Dall'Asta[3], Barbara G. Simpson[2], Andre R. Barbosa[4]

[1] School of Architecture and Design, University of Camerino
Viale della Rimembranza 3, 63100 Ascoli Piceno, Italy
e-mail: {laura.gioiella,michele.morici,alessandro.zona,fabio.micozzi}@unicam.it

[2] Civil and Environmental Engineering, Stanford University
473 Via Ortega, Stanford, CA 94305, USA
{mmcbain,bsimpson}@stanford.edu

[3] School of Science and Technology, University of Camerino
Via Gentile III da Varano 7, 62032 Camerino, Italy
andrea.dallasta@unicam.it

[4] School of Civil & Construction Engineering, Oregon State University
342 Owen Hall, Corvallis, OR 97331, USA
andre.barbosa@oregonstate.edu

Abstract

This study presents a vision-based methodology for acquiring absolute and inter-story displacements of multi-story buildings during dynamic and shake-table tests using only two video cameras. One camera is mounted on top of the building to track multiple targets positioned along the structure's height, while a second external camera provides redundancy for roof displacement measurements and compensates for noise caused by vibrations affecting the top-mounted camera. This setup enables the estimation of horizontal displacements across multiple floors. The methodology was validated through a full-scale 6-story building test on the Large High-Performance Outdoor Shake Table at the University of California San Diego. The results demonstrate high accuracy and resolution in displacement time series data.

Keywords: Absolute and Inter-story Displacement, Digital Image Correlation, Shake-Table Testing, Structural Health Monitoring, Vision-Based Monitoring.

1 INTRODUCTION

Shake-table testing is a crucial method in earthquake engineering, enabling the study of structural response under seismic excitation [1],[2]. Measuring displacements during such tests is challenging, as displacement sensors such as Linear Variable Displacement Transducers (LVDTs) and String Potentiometers (SPs) require fixed reference points, which are not always available, especially in large-scale tests [3]. An alternative approach involves double integration of accelerometer data [4], but this can introduce errors, particularly in inter-story drift estimations and residual displacements [5],[6].

To address these limitations, computer-vision emerged as a promising tool for direct displacement measurement [7]. This method allows frame-by-frame tracking of multiple points, even with a single camera, and can leverage cost-effective hardware. While vision-based systems were primarily used for bridges [8], their application to building monitoring, particularly in shake-table testing, grow, especially in the last five years [9]-[19]. Proposed approaches employed external cameras mounted on tripods [9]-[14] or UAVs [15], though some studies positioned cameras within the buildings being monitored [16]-[19]. However, these configurations often require multiple cameras, leading to increased setup complexity, synchronization challenges, and high computational demands for data processing. Additionally, motion compensation for UAV-mounted cameras and disturbances in internally placed cameras can affect measurement accuracy.

This study presents a novel and simplified vision-based methodology for measuring absolute and relative horizontal displacements in multi-story buildings during shake-table testing. It introduces a combined use of two strategically positioned cameras: one on the roof, capturing target displacements along the structure's height, and the other outside the building, providing redundant roof displacement measurements to compensate for motion-induced noise. Nevertheless, the application of the proposed approach is not confined to shake-table testing, possible applications cover different monitoring needs in the dynamic response of multi-story buildings, as is for example the case of push-and-release tests [20]. The proposed methodology was validated into two steps: first a simplified application on a 1-DOF desktop shake table was performed aiming at verifying the effectiveness of the Upsampling Cross-Correlation (UCC) algorithm [21] when used in environmental conditions. Successively, by applying it for the first application during the shake-table testing of a six-story mass timber building on the Large High-Performance Outdoor Shake Table (LHPOST6) at the University of California, San Diego. The results demonstrate that the proposed method offers a reliable and accurate alternative to traditional displacement monitoring techniques.

2 METHODOLOGY

The proposed vision-based methodology can be implemented either in a planar configuration with two cameras or in a three-dimensional setup using camera triplets. In both approaches, displacement extraction relies on the Upsampling Cross-Correlation (UCC) algorithm, which enables sub-pixel accuracy, up to 1/100 of a pixel, when high-contrast targets are used, such as chessboard-patterned squares with varying sizes and designs as in [22][23].

2.1 Planar configuration

The proposed methodology can be better understood by examining first its planar configuration with only two cameras, applied to a six-story building subjected to a unidirectional input (Figure 1). The internal camera is mounted at the roof corner, facing downward, and captures the motion of targets T0–T5 (represented by red lines in Figure 1), which are strategically designed and positioned to avoid overlapping during the movement of the building. Additionally,

this camera records the shake-table motion by measuring the displacement difference between T0 and T1, enabling a comparison with the controller response.

The second camera, an external one, is installed on the reaction mass at the ground floor (L0), acting as a fixed reference point. This camera solely tracks the roof displacement by monitoring the motion of the target T6, which is positioned near the internal camera. The roof-level displacement (L6) is, thus, recorded twice: once by the external camera via T6 and once by the internal camera via T0. In an ideal noise-free scenario, these measurements should be identical. Any discrepancies between them are caused by vibrations and rotations affecting the internal roof-mounted camera. The redundancy of the two cameras enables displacement correction, the noise introduced in the rooftop camera cab be obtained by subtracting the motion of T0 from that of T6. Subsequently, such noise can be used to correct the other readings obtained from the same rooftop camera.

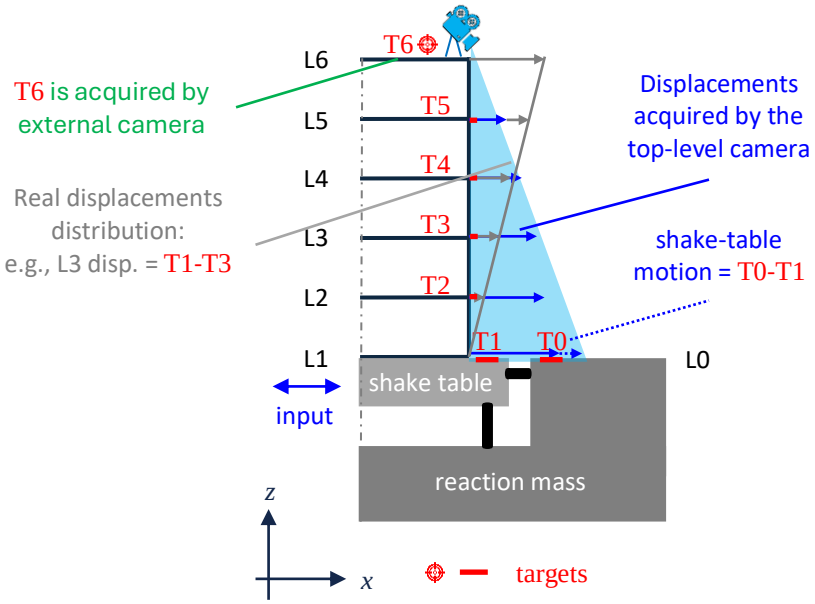

Figure 1: Basics of the proposed methodology during a monodirectional input in the shake table.

2.2 Three-dimensional configuration

The proposed configuration can be expanded to capture the motion of the building in three dimensions. To achieve this goal, two cameras are positioned at opposite corners of the building's roof to monitor multi-level horizontal displacements along the global x and y axes, as well as the movement of the shake table. Placing the cameras in these opposing positions improves data accuracy, particularly in cases where floor rotation occurs, assuming the floors behave as rigid diaphragms. The proposed setup ensures redundant displacement measurements across the widest possible horizontal distance. The two roof-mounted cameras, oriented downward, track multiple targets strategically sized and placed along the building's height to prevent overlapping during ground motion playback. In addition to the internal cameras, the vision-based system incorporates four external cameras, which serve two purposes: they provide redundant recordings of the roof-level horizontal displacements and help reduce data noise. The external cameras capture roof displacements by tracking two reference targets—one for each global axis (x and y)—positioned near the corresponding internal cameras.

3 PRELIMINAR APPLICATION ON A DESKTOP SHAKE-TABLE

Aiming at evaluating the efficiency of the UCC algorithm with light conditions proper of outdoor environments, as in the case of the full-scale tests performed at the LHPOST6, a simplified application was performed on an indoor 1-DOF desktop shake table. Both harmonic sinewaves and real ground motions were played back with and without light aiming at comparing time-histories of displacements acquired by the camera and by the controller. Since the controller of the desktop shake table provides also the response in terms of accelerations through double derivative of displacements, the same procedure was applied to the signals acquired by the cameras to have an estimation of the capability to acquire also time-series of accelerations, even though this is not the primary objective of the proposed methodology. Furthermore, the frequency contents of the signals of displacement provided by the controller and acquired by the camera were compared in the range 0 Hz-25 Hz.

The configuration used is depicted in Figure 2 and it encompasses a Teledyne FLIR BLACKFLY S BFS-U3-23S3M-C camera, with Tamron 23FM50SP lens having a focal length of 50 mm. The camera was installed on a tripod located at a distance D = 5 m from the desktop shake table. A single target of 20×20 mm, having pattern and square shape as suggested in [22],[23], installed on a steel "L" profile directly bolted on the shake table, was used. The dimension of the field of view (FOV) was 500x250 pixels, since ±60 mm of displacement was expected for all the tests, while an acquisition speed of 100 frames per second (FPS) was used. Figure 2 shows also the first frame of two video footages acquired with and without light to provide a quick insight on the effect of different light conditions.

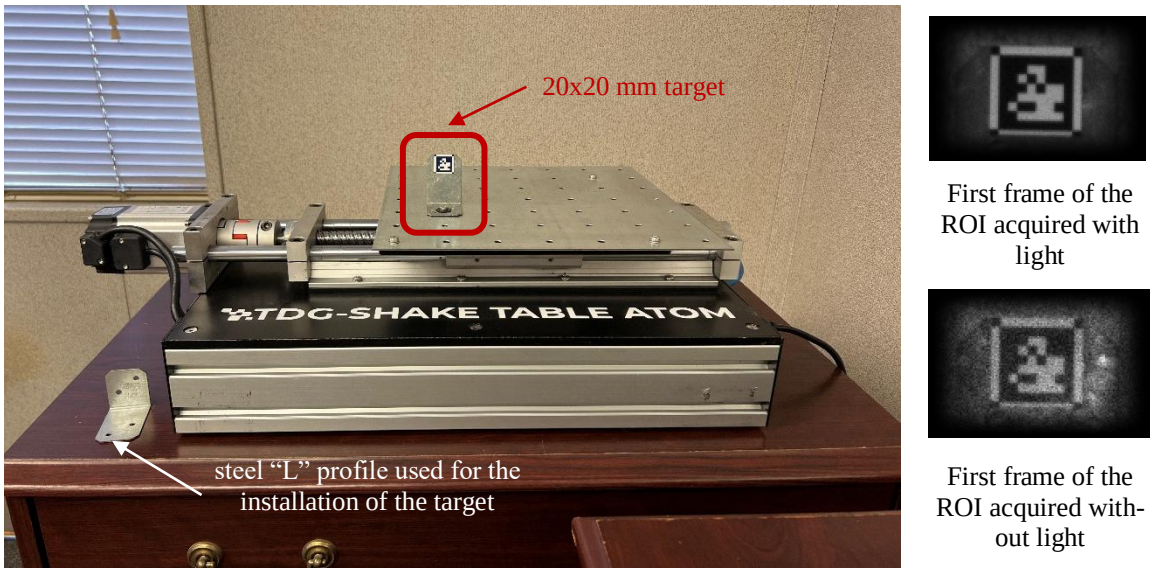

Figure 2: Desktop shake table: configuration under investigation.

Results described hereafter refer to a 2 Hz sinewave lasting 60 seconds and the ChiChi ground motion scaled to ensure analogous displacements as those produced by the waveform (±60 mm). The tests were repeated twice, with and without light.

Figure 3 compares the time-histories of displacements and accelerations recorded with and without light (orange and violet line, respectively) together with the controller data (green line) for the 2 Hz sinewave. It is worth noting that in both the conditions the algorithm can follow almost perfectly the path of the sinewave. Table 1 reports the highest positive and negative values of displacements and accelerations together with percentage errors evaluated in correspondence to positive and negative peak values. Generally, the acquisition performed with light

provided lower errors either in terms of displacement (2.20% instead of 2.27%) and of accelerations (7.12% versus 14.13%). For what concerns the accelerations, it is useful to underline that a 2 Hz sinewave leads to an acceleration of 0.965 g. Such value results also in the vibration of the desktop where the 1-DOF shake table was installed.

The bottom graph of Figure 3 reports the frequency contents of the displacement signals. The fundamental frequency of the input is perfectly recognized no matter what the environmental conditions are. The other peaks are in part related to the tripod of the camera, and probably to the fundamental frequencies of the desktop supporting the small shake-table.

Sine wave 2 Hz	Source	Max	min	Positive Peak Error [%]	Negative Peak Error [%]
Displacement [mm]	v-b without light	**60.50**	**-60.70**	1.91	**2.27**
	controller	59.37	-59.35		
	v-b with light	60.48	-60.67	1.86	**2.20**
	controller	59.38	-59.36		
Acceleration [g]	v-b without light	**1.047**	**-1.102**	8.42	**14.13**
	controller	0.965	-0.965		
	v-b with light	1.017	-1.034	5.30	**7.12**
	controller	0.965	-0.965		

Table 1: Desktop shake-table testing, statistics of the 2 Hz sinewave.

Figure 4 and Table 2 show results related to the ChiChi ground motion. Also in this case, the algorithm performed better with light than without, with the positive and negative peak errors that pass from 0.92% to 0.79% and from 1.19% to 1.09%, respectively, when considering displacements. It is worth observing that the path of displacements is perfectly recognized no matter what the light condition is, while the one in terms of accelerations is significantly noisier, especially without light. Moreover, the positive and negative errors are greater, especially without light (11.86% versus 7.52%, and 28.68% instead of 4.63%). Finally, the frequency content of the signals is overlapped in the range 0 Hz-7 Hz and very similar up to 25 Hz (upper bound value of the compared range).

ChiChi ground motion	Source	Max	min	Positive Peak Error [%]	Negative Peak Error [%]
Displacement [mm]	v-b without light	**57.74**	**-60.98**	0.92	**1.19**
	controller	57.22	-60.26		
	v-b with light	57.67	-60.92	0.79	**1.09**
	controller	57.21	-60.26		
Acceleration [g]	v-b without light	**0.255**	**-0.144**	11.86	**28.68**
	controller	0.228	-0.112		
	v-b with light	0.245	-0.117	**7.52**	4.63
	controller	0.228	-0.112		

Table 2: Desktop shake-table testing, statistics of the ChiChi ground motion.

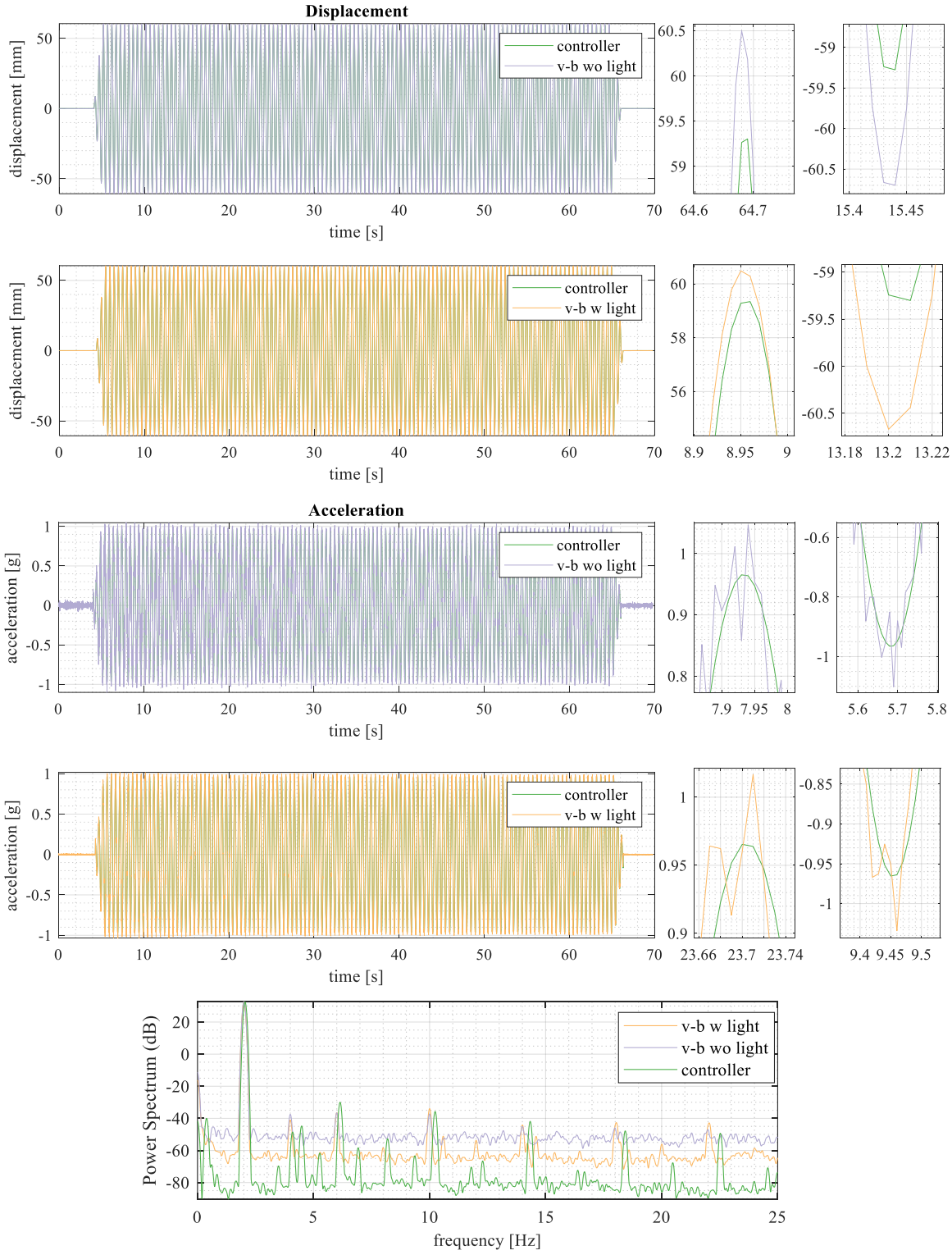

Figure 3: Desktop shake-table testing, results of the 2 Hz sinewave.

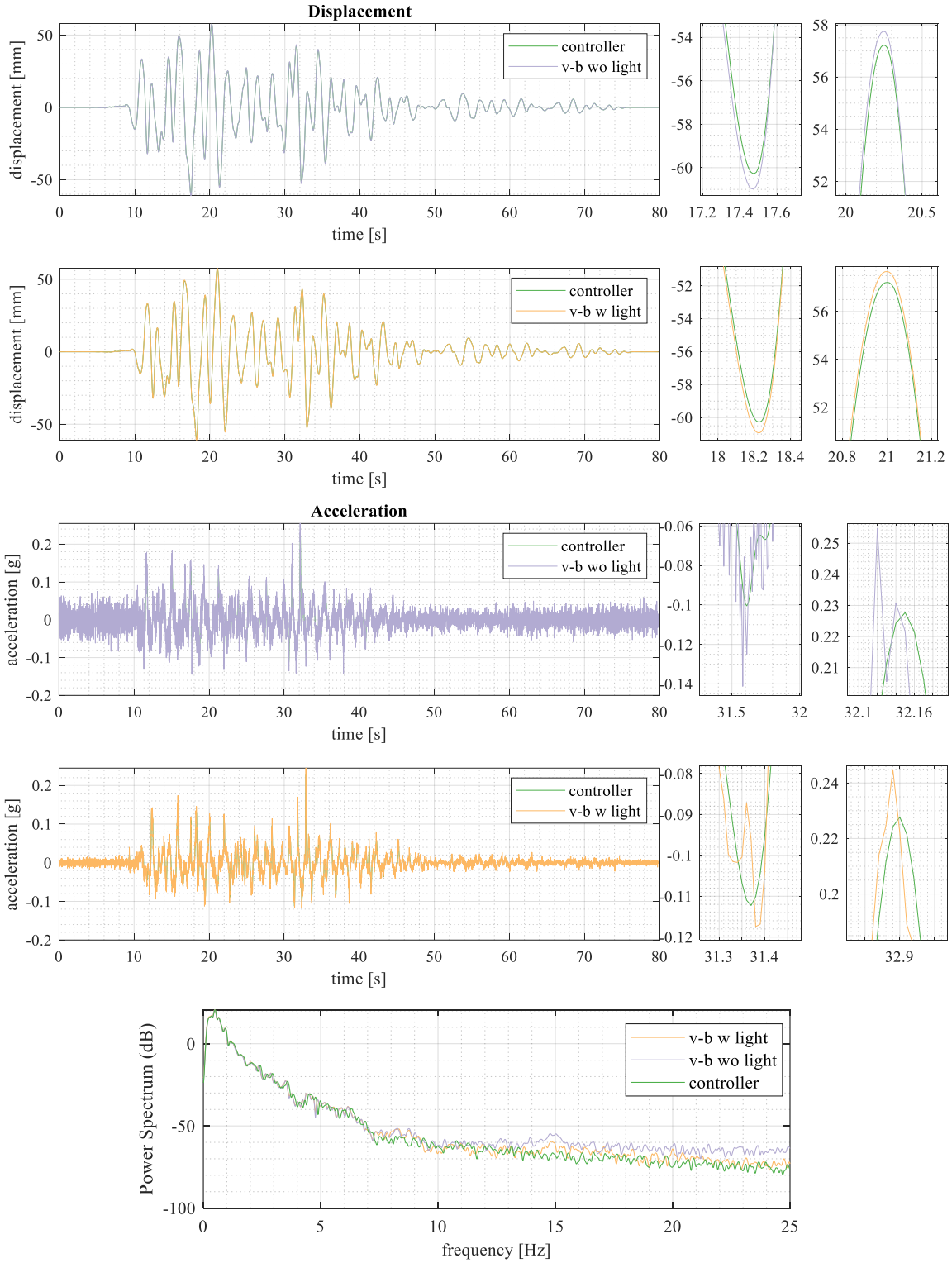

Figure 4: Desktop shake-table testing, results of the ChiChi ground motion.

4 FIRST APPLICATION TO A FULL-SCALE SHAKE-TABLE TESTING

This section reports few results related to the first application of the proposed methodology that took place in January 2024 at the LHPOST6 of the UCSD, with reference to the Maule Chile ground motion performed in the x-y directions simultaneously.

4.1 Testbed building and camera setup

The first implementation of the proposed vision-based methodology took place during Phase II of the NHERI Converging Design Project shake-table tests [24],[25]. The test specimen was a six-story mass timber building (Figure 5a) featuring a structural system composed of beams and columns with pinned connections supporting gravitational loads. Horizontal resistance was provided by four perimeter post-tensioned rocking walls, each incorporating a different lateral force-resisting system in the North-South (y) direction, tested separately across the three project phases. During Phase II, the lateral system consisted of Buckling-Restrained Braces (BRBs).

The goal of the vision-based methodology was to measure the building's displacements in the lateral (y) direction using only two video cameras, one internal and one external. The internal camera, referred to as the "roof camera," was mounted at the North-East corner of the roof (L7), facing downward. The external camera, labeled as the "ground camera," was positioned at ground level (L0), approximately 26 meters from the building's East side.

The FOV of each camera was determined based on multiple considerations, including: *i*) optical system characteristics; *ii*) floor-to-floor heights of the structure, corresponding to the sensor distances; *iii*) upsampling ratio (set to 100 in the proposed application) for the UCC algorithm; *iv*) expected displacement magnitudes; *v*) dimensions and numbers of targets as descending by the previous factors; *vi*) capability of the chosen laptop to handle the data stream from the camera sensor (one laptop per each camera).

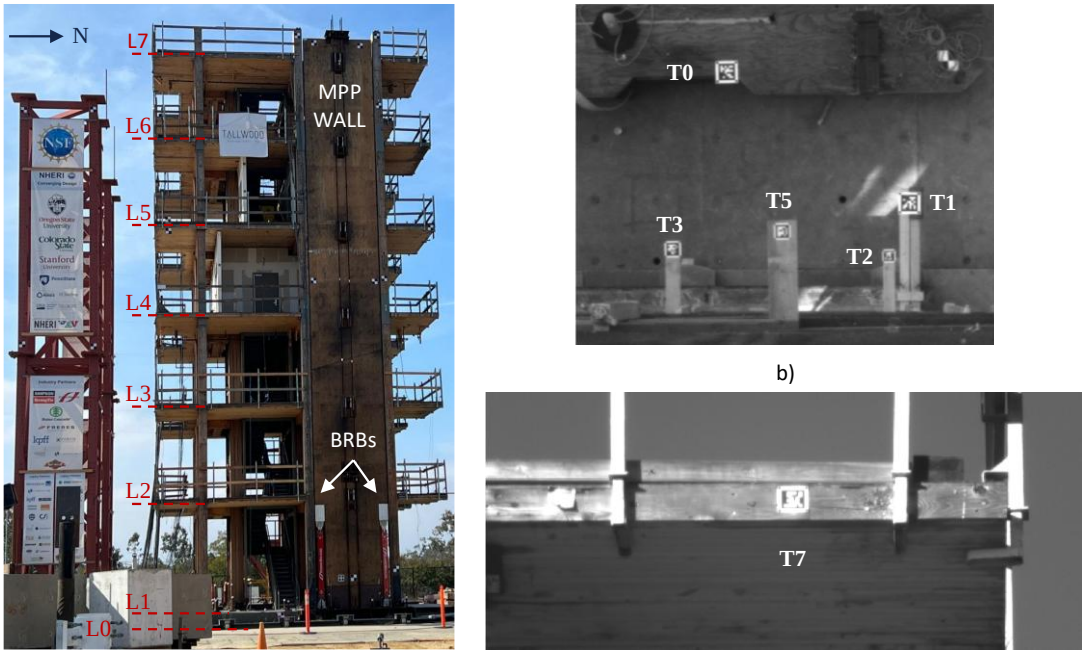

Figure 5: Testbed building (a); FOV and targets acquired by the roof camera (b) and by the ground camera (c).

Two Teledyne FLIR BLACKFLY S BFS-U3-23S3M-C cameras were employed, analogously to the one used for the 1-DOF desktop shake table, each linked to a laptop via USB3.0. The rooftop camera featured a lens with a 16 mm focal length. Its FOV was configured at 800 × 700 pixels (width × height) to capture the movement of targets positioned at levels L0 (reaction mass, size 200 mm × 200 mm), L1 (shake table, size 200 mm × 200 mm), L2 (elevation of +4.32 m, size 100 mm × 100 mm), L3 (+7.67 m, size 100 mm × 100 mm), and L5 (+14.38 m, size 50 mm × 50 mm). The displacements at L0 and L1 represent, respectively, the motion of the roof with and without shake-table motion. Since the ground-level camera records

only the lateral y-axis displacement of the roof to provide redundancy and mitigate potential noise, its FOV was set to 900 × 300 pixels, focusing on a single target (T7, 100 mm × 100 mm) located along the roof slab thickness (+21.08 m), with a lens of 50 mm focal length. Figure 5b) and Figure 5c) illustrate, respectively, the FOV and targets used for the rooftop and ground-mounted cameras. The recordings analysed in this research were captured at 100 FPS, a balance between hardware capacity, resulting size of the acquired videos, and expected performance, given the values of the other parameters (FOVs, ROIs, target dimensions).

4.2 Results from the Maule Chile ground motion playback

Over 50 playbacks constitute the sequence of tests conducted for phase II. Among these, the present article highlights specific outcomes related to the Maule Chile seismic excitation, applied in two dimensions at the intensity level of the Risk-targeted Maximum Considered Earthquake (MCEr), with a peak ground acceleration (PGA) in the lateral (y) direction of interest reaching 0.508 g.

The roof lateral displacement derived from the roof camera (T0) and the ground camera (T7) are compared in Figure 6. From the upper close-up that shows the first seconds of the motion, it can be noted that the signal acquired by the roof camera is notably disturbed as compared to the one acquired by the ground camera, because of the high frequency vibration induced by the shake table. The lower close-up shows, instead, that the noise is strongly reduced in the last part of the recordings (free vibration of the building) as the table is no longer working.

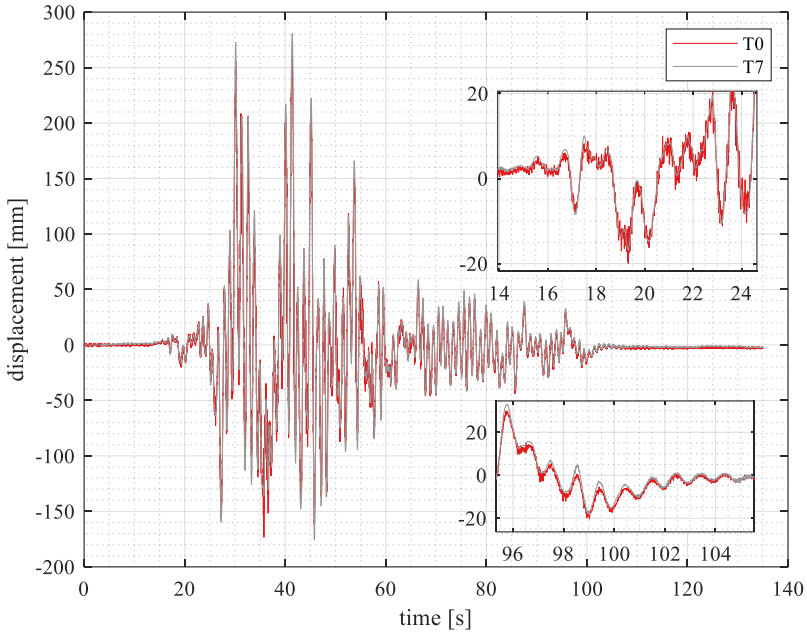

Figure 6: Full-scale shake-table testing under (Maule Chile ground motion playback), comparison of the roof lateral displacement derived from the roof camera (T0) and the ground camera (T7).

The platen longitudinal and lateral displacements measured by the shake-table controller (acquired at 512 Hz) and by the roof camera are compared in Figure 7. It is worth noting that, except for the resampling of the recording of the controller at the same frequency of the cameras (100 Hz) and alignment of the signals, no other treatment was done. Given that the displacements extracted from the roof camera are obtained as difference of displacements between two targets (T0 and T1) having nearly the same distance from the camera, the disturbance highlighted in the signal acquired by the roof camera, as shown for the target T0 in Figure 6, are

automatically compensated. This is confirmed by the close-ups in Figure 7, referring to the peak displacements, showing that the shake-table motion identified by the roof camera is almost free of noise, despite the significant disturbances induced by the high accelerations experienced on the roof (in the order of nearly 1 g).

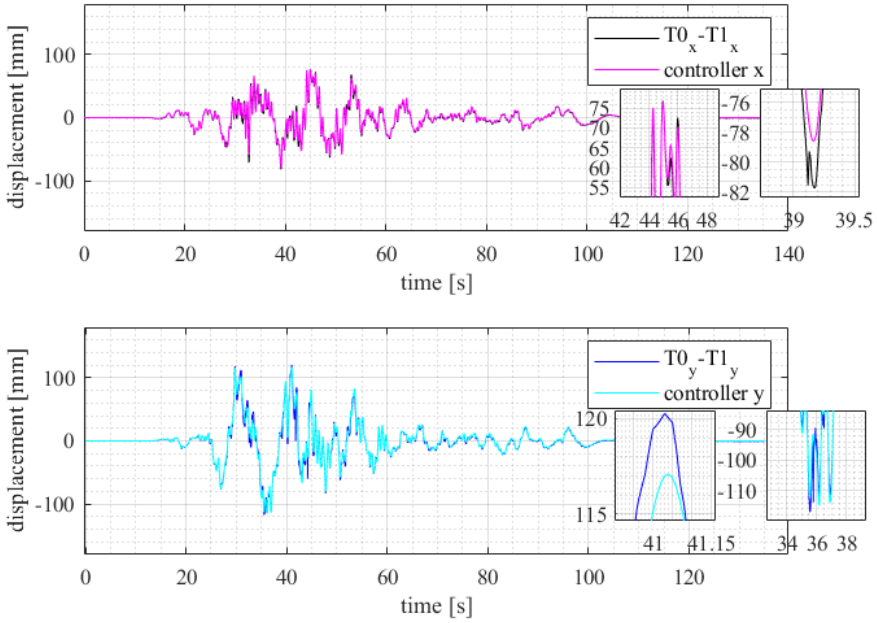

Figure 7: Full-scale shake-table testing under (Maule Chile ground motion playback), comparisons of the platen longitudinal and lateral displacements measured by the shake-table controller and by the cameras.

The peak values (positive and negative) of the platen displacement are reported in Table 3 to quantify the precision of the vision-based acquisition with respect to the controller, as described through the Root Mean Square Error (RMSE). Moreover, it is useful to also introduce the Normalized RMSE (RMSEN) that provides the same information in terms of percentage. The RMSE and RMSEN are, respectively, 3.15 mm and 12.35% (y direction) and 1.88 mm and 11.30% (x direction). By considering only the percentage errors calculated in correspondence of the highest positive and negative peak displacements, respectively, the values notably decrease to 2.72% and -1.84% for the y direction and 0.31% and 4.00% for the x. It is useful to remark that the response of the platen motion is referred to its Center of Mass (CoM), while the roof camera provided data referred to the Northeast corner (NE), consequently slight differences might be a consequence of building rotations.

Direction	Source	Max [mm]	min [mm]	RMSE [mm]	RMSEN [%]	Positive Peak Error [%]	Negative Peak Error [%]
y	roof cam.	120.28	-117.05	3.15	12.35	2.72	1.84
	controller	117.09	-114.93				
x	roof cam.	76.71	-81.73	1.88	11.30	0.31	4.00
	controller	76.47	-78.59				

Table 3: Full-scale shake-table testing under (Maule Chile ground motion playback), statistics of the shake-table motion acquired by roof camera and controller.

5 CONCLUSIONS

The application of the proposed vision-based methodology led to the following observations:

- The methodology exploits computer-vision to monitor displacements with a minimal number of video cameras, achieving highly accurate results compared to the shake-table controller's displacement readings.
- The combined use of internal and external cameras allows for the compensation of spurious displacements (noise) caused by vibrations affecting the internal camera during input motion playback.
- The methodology proves efficient, requiring fewer cameras compared to the large number of contact sensors typically used in testing, significantly reducing setup time.
- The proposed approach utilizes cost-effective hardware alongside highly efficient video processing software, with the potential for real-time extraction of displacement time histories at multiple points within the cameras' field of view.
- The UCC algorithm in combination with the squared chessboard targets are effective also in outdoor environmental conditions characterized by variable light conditions.

ACKNOWLEDGEMENTS

The Authors wish to thank Joel P. Conte at the University of California San Diego (UCSD) and the staff of the UCSD LHPOST6 for their support during testing. The Authors of the University of Camerino acknowledge funding by the European Union - NextGenerationEU, Mission 4, Component 2, under the Italian Ministry of University and Research (MUR) National Innovation Ecosystem grant ECS00000041 - VITALITY - CUPJ13C22000430001, the Italian Government, Fondo Complementare Programma unitario di intervento per le aree del terremoto del 2009 e 2016 Misura B - Sub-misura B.4 Centri di ricerca per l'innovazione Centro internazionale per la ricerca sulle Scienze e Tecniche dalla RICostruzione fisica, economica e sociale STRIC e STRIC+", and Fondazione ICSC, "HPC – National Centre for HPC, Big Data and Quantum Computing", Codice CN00000013, Spoke 5 "Environment & Natural Disasters" PNRR, Missione 4, Componente 2, Investimento 1.4 – European Union – NextGenerationEU; CUP H93C22000450007, project FABRICH.

REFERENCES

[1] Van Den Einde L, Conte JP, Restrepo JI, Bustamante R, Halvorson M, Hutchinson TC, Lai CT, Lotfizadeh K, Luco JE, Morrison ML, Mosqueda G, Nemeth M, Ozcelik O, Restrepo S, Rodriguez A, Shing PB, Thoen B, Tsampras G. (2021) NHERI@UC San Diego 6-DOF Large High-Performance Outdoor Shake Table Facility. Front. Built Environ. 6:580333

[2] Nakashima M, Nagae T, Enokida R, et al. (2018) Experiences, accomplishments, lessons, and challenges of E-defense—Tests using world's largest shaking table. Japan Archit Rev 1(1):4–17.

[3] Pei S, Ryan KL, Berman JW, Van De Lindt JW, Pryor S, Huang D, Wichman S, Busch A, Roser W, Wynn SL, Ji Y, Hutchinson T, Sorosh S, Zimmerman RB, Dolan J. (2024)

Shake-Table Testing of a Full-Scale 10-Story Resilient Mass Timber Building. J. Struct. Eng. 150(12):04024183.

[4] Bock Y, Melgar D, and Crowell BW. (2011) Real-time strong-motion broadband displacements from collocated GPS and accelerometers. Bulletin of the Seismological Society of America, 101(6):2904-2925.

[5] Skolnik DA, Wallace JW. (2010). Critical Assessment of Interstory Drift Measurements. J. Struct. Eng. 136(12):1574–1584

[6] Dai Z, Li X, Chen S, et al. (2020) Baseline correction based on L1-Norm optimization and its verification by a computer vision method. Soil Dyn Earthq Eng 131:106047

[7] Feng D, Feng MQ. (2021) Computer Vision for Structural Dynamics and Health Monitoring. New York: Wiley

[8] Zona A. (2021) Vision-Based Vibration Monitoring of Structures and Infrastructures: An Overview of Recent Applications. Infrastructures 6(1):4.

[9] Ngeljaratan L, Moustafa MA. Structural health monitoring and seismic response assessment of bridge structures using target-tracking digital image correlation. Engineering Structures 213(1):110551.

[10] Wang J, Zaho J, Yuwen L, Shan J. (2021) Vision-based displacement and joint rotation tracking of frame structure using feature mix with single consumer-grade camera. Structural Control Health Monitoring 28(12):e2832

[11] Choi I., Kim J, Sohn J. (2022) Automated framework for monitoring building structures through derivation of lateral stiffness using marker-free vision-based displacement sensor. Measurement 194(1):111062.

[12] Ji X, Gao X, Zhuang Y, Qu Z. (2023) Enhanced measurements of structural inter-story drift responses in shaking table tests. Engineering Structures 278(1):115508.

[13] Pan X, Yang TY, Xiao Y, Yao H, Adeli H (2023) Vision-based real-time structural vibration measurement through deep-learning-based detection and tracking methods. Engineering Structures 281(1):115676

[14] Sun PP, Vasef M, Chen L. (2025) Multi-vision-based displacement monitoring using global-local deep deblurring and Rauch-Tung-Striebel smoother. Measurement 242(E): 116292.

[15] Wang X, Lo E, De Vivo L, Hutchinson TC, Kuester F. (2022) Monitoring the earthquake response of full-scale structures using UAV vision-based techniques. Structural Control and Health Monitoring 29(1):e2862.

[16] Park JW, Lee JJ, Jung HJ, Myung H. (2010) Vision-based displacement measurement method for high-rise building structures using partitioning approach. NDT & E International 43(7):642–647.

[17] Petrone F, Perez R, Coates J, McCallen D. (2023) A Biaxial Discrete Diode Position Sensor for Rapid Postevent Structural Damage Assessment. J. Struct. Eng. 149(3):11776.

[18] Harvey Jr PS, Elisha G. (2018) Vision-based vibration monitoring using existing cameras installed within a building. Structural Control Health Monitoring 25:e2235

[19] Zhou J, Huo L, Huang C, Yang Z, Li H. (2024) Feasibility study of earthquake-induced damage assessment for structures by utilizing images from surveillance cameras. Structural Control Health Monitoring 4993972.

[20] Dall'Asta A, Leoni G, Gioiella L, Micozzi F, Ragni L, Morici M, Scozzese F, Zona A. (2022) Push-and-release tests of a steel building with hybrid base isolation. Engineering Structures 272(1):114971.

[21] Guizar-Sicairos M; Thurman ST, Fienup JR. (2008) Efficient subpixel image registration algorithms. Opt. Lett 33:156–158

[22] Micozzi F, Morici M, Zona A, Dall'Asta A. (2023) Vision-Based Structural Monitoring: Application to a Medium-Span Post-Tensioned Concrete Bridge under Vehicular Traffic. Infrastructures 8(10):152

[23] Micozzi F, Morici M, Zona A, Dall'Asta A. (2024) Vision-based dynamic monitoring of a post-tensioned concrete bridge under vehicular traffic. Procedia Structural Integrity 62C:848-855.

[24] https://tallwoodinstitute.org/converging-design-home-5663/

[25] Barbosa A, Simpson B, van de Lindt J, Sinha A, Field T, McBain M, Uarac P, Kontra S, Mishra P, Gioiella L, Pieroni L, Pryor S, Saxey B. (2025) "Shake table testing program for mass timber and hybrid resilient structures datasets for the NHERI Converging Design project", in Shake table testing program of 6-story mass timber and hybrid resilient structures (NHERI Converging Design project). DesignSafe-CI